PHYSICAL REVIEW C **89**, 011303(R) (2014)

Microscopic description of translationally invariant core + N + N overlap functions

D. Sääf and C. Forssén*
Department of Fundamental Physics, Chalmers University of Technology, SE-412 96 Göteborg, Sweden
(Received 2 October 2013; revised manuscript received 5 December 2013; published 10 January 2014)

We derive expressions for core $+N+N$ overlap integrals starting from microscopic wave functions obtained in the *ab initio* no-core shell model. These overlap integrals correspond to three-body channel form factors and can be used to investigate the clustering of many-body systems into a core plus two nucleons. We consider the case when the composite system and the core are described in Slater determinant, harmonic oscillator bases, and we show how to remove spurious center-of-mass components exactly in order to derive translationally invariant overlap integrals. We study in particular the Borromean ^{6}He nucleus using realistic chiral nuclear interactions, and we demonstrate that the observed clusterization in this system is a Pauli focusing effect. The inclusion of three-body forces has a small effect on this structure. In addition, we discuss the issue of absolute normalization for spectroscopic factors, which we show is larger than one. As part of this study we also perform extrapolations of ground-state observables and investigate the dependence of these results on the resolution scale of the interaction.

DOI: 10.1103/PhysRevC.89.011303 PACS number(s): 21.10.Jx, 21.30.Fe, 21.60.De, 27.20.+n

Introduction. The structure of light nuclei is a very rich subject. A particularly interesting phenomenon is the importance of clusterization. Cluster structures appear frequently around reaction thresholds and are manifested, e.g., in large cluster form factors [1]. It is often modeled by assuming that intrinsic cluster degrees of freedom are frozen, thus reducing the full many-body problem to an effective few-body one. However, the appearance of clusterization from a microscopic perspective remains to be elucidated [2–4]. It is not clear how strong short-range correlations, induced by realistic nuclear forces, propagate to longer-range cluster structures. In addition, given the fermionic nature of nucleons we can be sure that antisymmetrization at the many-body level will always play an important role.

For light nuclei we have seen major progress in the development of *ab initio* approaches [5–7]. The state-of-the-art methods are based on controlled approximations and the underlying computational schemes account for successive many-body corrections in a systematic way [8]. Recently, the application of chiral effective field theory (EFT) [9–12] and renormalization-group techniques [13] has resulted in a systematic approach to the nuclear interaction.

Even more recently, *ab initio* approaches began to bridge the gap from nuclear structure to reactions [14–17]. Direct reactions, such as stripping and pickup of a single nucleon, constitute a current frontier for these methods. In contrast, there exists a rather standard approximation to treat such reactions within phenomenological models [18] that uses spectroscopic factors as input parameters [1,19,20]. The spectroscopic factor corresponds to the integrated norm of the cluster form factor. From a microscopic perspective it is a purely theoretical construct that is defined from wave function overlaps. It is expected that a correct treatment of translational invariance will be important for this quantity. The particular case of three-body channels in ^{6}He was studied by Timofeyuk [21], who found a significant increase of the normalization when using a translation-invariant shell model. This observation was verified by Brida and Nunes [22] using a microscopic Monte Carlo approach with schematic interactions.

In this Rapid Communication we derive algebraic expressions for calculating translationally invariant cluster form factors from no-core shell-model (NCSM) wave functions. We restrict ourselves to three-body core $+N+N$ channels, and we will apply our formalism to study ^{4}He $+n+n$ cluster structures in the Borromean system ^{6}He [23]. Despite its short β-decay lifetime, a series of precision measurements on ^{6}He ground-state properties have recently been performed. Its binding energy was measured using the TITAN Penning trap mass spectrometer [24], and its charge radius was determined from laser spectroscopy [25,26]. In addition, there are several theoretical studies of ^{6}He in the literature, ranging from from inert cluster models [23,27] and microscopic methods [22,28–30] with phenomenological or semirealistic interactions to *ab initio* approaches [31–34] using high-precision nuclear interactions.

The structure of this Rapid Communication is as follows. First we give a brief introduction to the NCSM and we present the derivation of algebraic expressions for core $+N+N$ channel form factors. Then we present our results for ground-state properties of ^{6}He using chiral interactions. Then we turn to the overlap of ^{6}He with ^{4}He $+n+n$. We plot the correlation density and decompose the cluster form factor into different components of a hyperspherical harmonics expansion. Finally, we present a discussion of our results and also give an outlook.

Theoretical formalism. In the NCSM we consider a system of A pointlike nonrelativistic nucleons. The many-body basis is constructed from Slater determinants (SD) of harmonic oscillator (HO) single-particle states. A basis truncation is introduced by including all HO configurations up to a certain energy cutoff (defined by the parameter $N_{\max}$). This particular choice of basis truncation guarantees translational invariance as all eigenstates will factorize into a product of a state depending on intrinsic coordinates and a state depending only on the center-of-mass (CM) coordinate. Eigensolutions

*christian.forssen@chalmers.se

with spurious CM excitations can then be shifted up in the spectrum by adding a Lawson projection term [35] to the Hamiltonian. The NCSM Hamiltonian contains realistic two- and three-body nuclear interactions, and the resolution scale of the Hamiltonian matrix is usually lowered with similarity transformations. See, e.g., Ref. [5] for a more detailed description of the NCSM method.

Since we want to compute a translationally invariant cluster form factor, but still work with wave functions expressed in the NCSM basis with single-particle coordinates, we need to take special care to remove spurious CM components. A framework for performing this was introduced in [36] and is here generalized to the case of three-body core $+N+N$ channels.

We define the following set of Jacobi coordinates for an A-nucleon system, adopting the notation of [36], where $\vec{\xi}_0$ is the A-body CM coordinate and $\boldsymbol{\xi}$ is the set of normalized Jacobi coordinates for the $A-2$ particles in the core. The relative coordinates for the clusters are defined as

$$\vec{\eta} = \sqrt{\frac{2(A-2)}{A}}\left[\frac{1}{A-2}\sum_{i=1}^{A-2}\vec{r}_i - \frac{1}{2}(\vec{r}_{A-1}+\vec{r}_A)\right], \quad (1a)$$

$$\vec{\nu} = \sqrt{\frac{1}{2}}[\vec{r}_{A-1}-\vec{r}_A], \quad (1b)$$

which correspond to the normalized "T-coordinate" system of core $+N+N$. Using this set of Jacobi coordinates we define cluster-separated A-nucleon wave functions, which will be equivalent to a basis set in the continuous variables (η,ν). Each basis function corresponds to a set of frozen relative distances, which is reflected by two Dirac δ functions

$$\begin{aligned}\left\langle \boldsymbol{\xi}\eta'\vec{\eta}\nu'\vec{\nu}\boldsymbol{\sigma}\boldsymbol{\tau}\middle|\Phi^{AJMTM_T}_{\alpha M_\alpha};\delta_\eta\delta_\nu\right\rangle &= \sum (l_\eta m_\eta l_\nu m_\nu|LM_L)(I_2M_2I_3M_3|I_{23}M_{23})(I_1M_1I_{23}M_{23}|SM_S)(LM_LSM_S|JM)\\ &\times \left(T_2M_{T_2}T_3M_{T_3}\middle|T_{23}M_{T_{23}}\right)\left(T_1M_{T_1}T_{23}M_{T_{23}}\middle|TM_T\right)\frac{\delta(\eta-\eta')}{\eta\eta'}\frac{\delta(\nu-\nu')}{\nu\nu'}Y_{l_\eta m_\eta}(\hat{\eta})Y_{l_\nu m_\nu}(\hat{\nu})\\ &\times \left\langle\sigma_{A-1}\tau_{A-1}\middle|\ I_2M_2T_2M_{T_2}\right\rangle\left\langle\boldsymbol{\xi},\sigma_1\ldots\sigma_{A-2},\tau_1\ldots\tau_{A-2}\middle|\ (A-2)\alpha_1I_1M_1T_1M_{T_1}\right\rangle, \end{aligned} \quad (2)$$

where $\boldsymbol{\sigma}=\sigma_1,\ldots,\sigma_A$ and $\boldsymbol{\tau}=\tau_1,\ldots,\tau_A$ are the spin and isospin coordinates of the A nucleons, and $\alpha\equiv\{\alpha_1I_1T_1,I_2T_2,I_3T_3;LS\}$ denotes the three-body channel in LS coupling with the corresponding projection quantum numbers M_α. The core, with $A-2$ nucleons, has total angular momentum I_1 and isospin T_1, while α_1 correspond to additional quantum numbers needed to characterize the eigenstate. Particles 2 and 3 are single nucleons, so $I_2=I_3=T_2=T_3=1/2$. The A-body system has a total angular momentum J and a total isospin T with projections M and M_T, respectively.

The core $+N+N$ three-body channel form factor for an A-body state λJT, with λ denoting additional quantum numbers necessary to characterize the state, can be defined as the overlap integral

$$u^{A\lambda JT}_\alpha(\eta,\nu) = \left\langle A\lambda JT\middle|\mathcal{A}_{A-2,1,1}\Phi^{AJT}_\alpha;\delta_\eta\delta_\nu\right\rangle = \sum_{n_\eta,n_\nu}\sqrt{\frac{A!}{(A-2)!}}R_{n_\eta l_\eta}(\eta)R_{n_\nu l_\nu}(\nu)\left\langle A\lambda JT\middle|\Phi^{AJT}_\alpha;n_\eta l_\eta,n_\nu l_\nu\right\rangle, \quad (3)$$

where $\mathcal{A}_{A-2,1,1}$ is a cluster antisymmetrizer. It permutes particles between the clusters and gives a simple combinatorial factor when acting on the fully antisymmetrized bra state. In this expression we have expanded the Dirac δ functions in terms of radial HO functions, R_{nl}, defined with the HO length parameter $b=\sqrt{\hbar/m\Omega}$, with m the nucleon mass and Ω the HO frequency. The new basis functions $\langle\boldsymbol{\xi}\vec{\eta}\vec{\nu}\boldsymbol{\sigma}\boldsymbol{\tau}|\Phi^{AJMTM_T}_{\alpha M_\alpha};n_\eta l_\eta,n_\nu l_\nu\rangle$ are identical to Eq. (2), but with the delta functions replaced by HO functions $R_{n_\eta l_\eta}(\eta)R_{n_\nu l_\nu}(\nu)$. The spectroscopic factor is the norm of the overlap integral.

The relationship between an A-nucleon wave function expressed in the SD basis, with $0S$ CM motion as guaranteed by the Lawson projection, and the corresponding state in Jacobi coordinates is

$$\langle\vec{r}_1\ldots\vec{r}_A\boldsymbol{\sigma}\boldsymbol{\tau}|\ A\lambda JMTM_T\rangle_{\rm SD} = \langle\boldsymbol{\xi}\vec{\eta}\vec{\nu}\boldsymbol{\sigma}\boldsymbol{\tau}|\ A\lambda JMTM_T\rangle\,\psi_{000}(\vec{\xi}_0). \quad (4)$$

By applying this relationship to the composite and cluster states it is possible to relate the overlap in Jacobi coordinates with an overlap expressed in an SD basis,

$$\left\langle A\lambda JT\middle|\ \mathcal{A}_{A-2,1,1}\Phi^{AJT}_\alpha;n_\eta l_\eta,n_\nu l_\nu\right\rangle = \frac{{}_{\rm SD}\left\langle A\lambda JT\middle|\ \mathcal{A}_{A-2,1,1}\Phi^{AJT}_\alpha;n_\eta l_\eta,n_\nu l_\nu\right\rangle_{\rm SD}}{\left\langle n_\eta l_\eta 00 l_\eta\middle|\ 00 n_\eta l_\eta l_\eta\right\rangle_{\frac{2}{A-2}}}, \quad (5)$$

where the denominator is the general HO bracket [37] that results from a Talmi-Moshinksky transformation. A second transformation takes us from η and ν to single-particle coordinates (subscripts a and b) for the two nucleons outside the core. Finally, recoupling spins and integrating over the intrinsic coordinates we arrive at an expression for the form factor

expressed in terms of double-reduced matrix elements between SD eigenstates,

$$u_\alpha^{A\lambda JT}(\eta,\nu) = \sum_{\substack{n_\eta l_\eta \\ n_\nu l_\nu \cdots}} \frac{R_{n_\eta l_\eta}(\eta) R_{n_\nu l_\nu}(\nu)}{\langle n_\eta l_\eta 00 l_\eta | 00 n_\eta l_\eta l_\eta \rangle_{\frac{2}{A-2}}} (-1)^{3I_1+I_{23}+J_{ab}-T_{23}-S+L} \langle n_a l_a n_b l_b L | n_\eta l_\eta n_\nu l_\nu L \rangle_1$$

$$\times \frac{\hat{L}\hat{S}\hat{J}_{ab}^2 \hat{j}_a \hat{j}_b}{\hat{J}\hat{T}} \begin{Bmatrix} L & I_{23} & J_{ab} \\ I_1 & J & S \end{Bmatrix} \begin{Bmatrix} l_a & l_b & L \\ I_3 & I_2 & I_{23} \\ j_a & j_b & J_{ab} \end{Bmatrix} {}_{\rm SD}\langle A\lambda JT \| \left[a^\dagger_{n_a l_a j_a t_a} a^\dagger_{n_b l_b j_b t_b} \right]^{J_{ab} T_{ab}} \| (A-2)\alpha_1 I_1 T_1 \rangle_{\rm SD}, \quad (6)$$

where J_{ab} (T_{ab}) is the coupled total spin (isospin) of the two nucleons. The $a^\dagger a^\dagger$ matrix elements are calculable by using a special version of our transition density code [36].

Results. We will start this section with a presentation of our results for ^{6}He ground-state observables. We will then extract the three-body channel form factors and the corresponding spectroscopic factors. Our calculations are performed in the NCSM for model spaces up to $N_{\rm max} = 16$, corresponding to a basis dimension of 3.6×10^8. Unless otherwise stated, we employ the Idaho chiral *NN* interaction at next-to-next-to-next-to-leading order (N^{3}LO) with a 500-MeV regularization cutoff [11]. The interaction is evolved in the two-body free space using the Similarity Renormalization Group (SRG) flow equation [13] in order to compute a phase-shift equivalent, effective two-body interaction. We note that the truncation of the evolution at two-body level will impose a violation of formal unitarity for the transformation in the many-body space. A specific aim of this study is therefore to investigate the dependence of our results on the SRG flow parameter $\Lambda_{\rm SRG}$. We will use a physically motivated range of resolution scales, corresponding to $\Lambda_{\rm SRG} = 1.8$–2.2 fm^{-1}.

For any choice of realistic interaction, the ground-state energy of a many-body system calculated in a truncated space shows a dependence on the basis parameters $N_{\rm max}$ and $\hbar\Omega$. By construction, our results should be independent of $\hbar\Omega$ in the limit of infinite model space. We will now discuss extrapolations of our ^{6}He finite-space results. Our oscillator basis truncation can be translated into corresponding infrared (IR) and ultraviolet (UV) cutoffs [38–40]. Following Refs. [39,40], we define the UV momentum cutoff $\Lambda_{\rm UV} = \sqrt{2(N+3/2)}\hbar/b$, where N is the truncation in the single-particle basis ($N = N_{\rm max} + 1$ for p-shell nuclei). For the IR parameter we use $\Lambda_{\rm IR} = 1/L$, with $L = L_2 \equiv \sqrt{2(N+3/2+2)}b$ as suggested in Ref. [40]. Working in very large model spaces, we are able to capture the UV physics of the softened interaction. As a consequence, the IR correction will be the most important one and we use the IR dependence of the energy that was derived in Ref. [39],

$$E_L = E_\infty + Ae^{-2k_\infty L}, \quad (7)$$

where k_∞ should be related to the binding momentum, but in practice will be used as a free fit parameter together with A and the desired E_∞. In addition, we use the suggested IR correction formula for the point-proton radius [39],

$$\langle r^2 \rangle_L \approx \langle r^2 \rangle_\infty [1 - (c_0\beta^3 + c_1\beta)e^{-\beta}], \quad (8)$$

where $\beta \equiv 2k_\infty L$. We use c_0, c_1, and $\langle r^2 \rangle_\infty$ as fit parameters, but we keep k_∞ fixed from the energy fit. Our calculated data for these two ground-state observables are presented in Fig. 1 together with the extrapolation curves.

In practice, we want to test the performance of the extrapolation procedure as a function of the model space truncation. We start by imposing a rather small $N_{\rm max}$ truncation and collect the results computed at the largest values of $\Lambda_{\rm UV}$ into one data set of five points that is used for the curve fit. The error bar reflects the variance from the least-squares fit. It does not include an estimate of the systematic error from the extrapolation. This procedure is then repeated for increasing $N_{\rm max}$, i.e., including more data, until we finally use the unrestricted data set. The evolution of the extrapolated result with error bars from $N_{\rm max} \leqslant 10$–16 is shown in Fig. 1. While we find a consistent set of results for the energies, we note that there is a trend of increasing point-proton radius that calls for further investigation. Final results, obtained with the unrestricted data set $N_{\rm max} \leqslant 16$, are presented in Table I for three different SRG parameters. The fact that the unitarity of the transformation is only approximate leads to binding and separation energy variations of a few hundred keV but is hardly noticeable within error bars of the extrapolated radius.

Next we turn to the computation of three-body channel form factors from our microscopic wave functions. We employ Eq. (6) with NCSM wave functions up to $N_{\rm max} = 14$. In Fig. 2 we show the main ($L = S = 0$) component of the $\langle ^6\text{He}(0^+) | ^4\text{He}(0^+) + n + n \rangle$ overlap and the much smaller $L = S = 1$ component. Our microscopic calculation provides a beautiful confirmation of the two-peak structure of this form factor, as reported in earlier phenomenological cluster model studies [23,27,42], and within a microscopic model with schematic interactions [22]. It is clear that the small $L = S = 1$ component does not show any signs of a similar structure.

Now we are uniquely positioned to analyze this form factor behavior and to understand the origin of the observed clustering. To begin with, we note that the so called dineutron configuration has the largest peak probability. This is expected since it contributes to a shift of the position of the charged core with respect to the total center of mass, and therefore to an increased charge radius, which is consistent with experimental findings. Note, however, that the average distance between the two neutrons is not very small ($\sim$2 fm), and it can be expected that the influence on the charge radius will diminish when adding additional neutrons. Indeed, it has been shown experimentally that the charge radius increases for ^{6}He, but

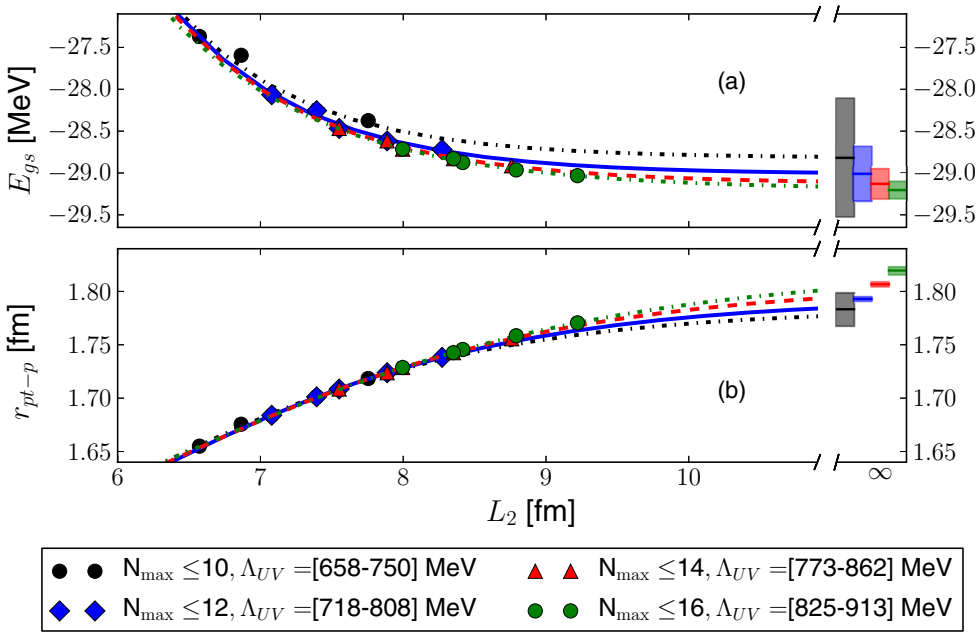

FIG. 1. (Color online) Extrapolation of ^{6}He binding energy (a) and point-proton radius (b) as a function of the IR cutoff parameter. Results are obtained with the NCSM using an SRG-evolved chiral two-body interaction ($\Lambda_{\rm SRG} = 2.0$ fm^{-1}). See text for details on the extrapolation procedure.

it decreases again in ^{8}He [24]. Gamow shell-model calculations [27], which incorporate continuum structures explicitly, confirm that the amplitude of the dineutron configuration is reduced when going from ^{6}He to ^{8}He.

We claim that the origin for the observed cluster structure in ^{6}He is the Pauli principle. To substantiate this statement we show in Fig. 3 a sequence of contour plots obtained at $N_{\rm max} =$ 2, 8, and 14. The same structure is clearly seen in all three panels, although the former ones represent calculations that are far from converged; i.e., the model space is much too small to accommodate the correlations induced by the interaction. However, what is present already at the smallest model spaces is the correct antisymmetrization. The importance of a proper treatment of antisymmetrization was stressed in previous microscopic studies (see, e.g., Ref. [22]). Obviously, this feature remains a very weak point in models with inert clusters. The wave function obtained with a three-body Hamiltonian (SRG-evolved chiral two- plus three-nucleon forces ($NN + 3NF$) [43]) exhibits the same clusterization structure, as can be observed in the lower right panel of Fig. 3.

In order to analyze the cluster form factors further we have performed a projection on hyperspherical harmonics (HH) basis functions. The hypercoordinates $(\rho,\theta,\hat{\eta},\hat{\nu})$ are related to the Jacobi coordinates $(\vec{\eta},\vec{\nu})$ via $\eta = \rho\cos\theta$, $\nu = \rho\sin\theta$. The cluster form factor from Eq. (6), expressed in (ρ,θ) coordinates, can be projected onto the HH basis

$$u_\alpha^{A\lambda JT}(\theta,\rho) = \frac{1}{\rho^{5/2}} \sum_{K,l_\eta,l_\nu} \chi_{\alpha,Kl_\eta l_\nu}^{A\lambda JT}(\rho)\psi_K^{l_\eta,l_\nu}(\theta), \qquad (9a)$$

where

$$\chi_{\alpha,Kl_\eta l_\nu}^{A\lambda JT}(\rho) = \rho^{5/2}\int_0^{\frac{\pi}{2}} d\theta' \sin^2\theta'\cos^2\theta'\psi_K^{l_\eta,l_\nu *}(\theta') \times \sum_{n_\eta,n_\nu} C_{\alpha,n_\eta l_\eta,n_\nu l_\nu}^{A\lambda JT} R_{n_\eta l_\eta}(\theta',\rho)R_{n_\nu l_\nu}(\theta',\rho), \qquad (9b)$$

and where $\psi_K^{l_\eta,l_\nu}(\theta)$ is the hyperangular basis function [44], and the last row is a compact formulation of the right-hand side of Eq. (6).

TABLE I. Extrapolated results for the ^{6}He binding energy, two-neutron separation energy, and point-proton radius. Results are obtained with the NCSM using an SRG-evolved chiral two-body interaction with three different SRG flow parameters. The last column shows theoretical results from Bacca *et al.* [32] using the hyperspherical-harmonics approach with the same chiral interaction, but employing the $V_{\text{low }k}$ renormalization technique.

	Experiment [24]	This work			Bacca *et al.* [32,41]
		$\Lambda_{\rm SRG} = 1.8$	$\Lambda_{\rm SRG} = 2.0$	$\Lambda_{\rm SRG} = 2.2$	$V_{\text{low }k}$ ($\Lambda = 2.0$ fm^{-1})
$E_{\rm gs}$ (MeV)	29.269	29.67(3)	29.20(11)	28.61(22)	29.47(3)
S_{2n} (MeV)	0.975	1.22(2)	0.95(10)	0.68(22)	0.82(4)
$r_{\text{pt-p}}$ (fm)	1.938(23)	1.820(4)	1.820(4)	1.815(8)	1.804(9)

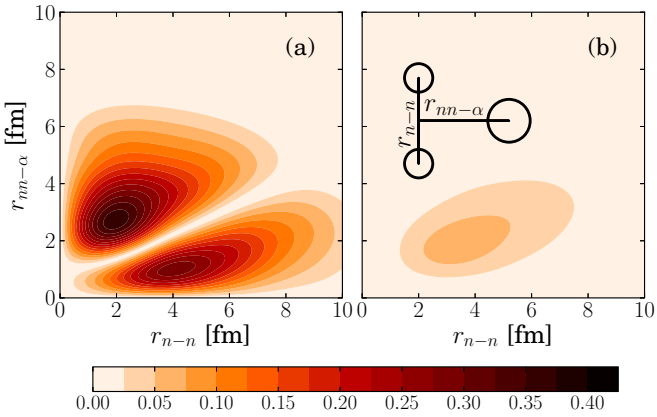

FIG. 2. (Color online) Contour plots of the translationally invariant three-body channel form factor $\langle {}^6\mathrm{He}(0^+)|{}^4\mathrm{He}(0^+)+n+n\rangle$ calculated from NCSM wave functions. The two allowed channels for this overlap, $L=S=0$ and $L=S=1$, are shown in panels (a) and (b), respectively.

In Fig. 4 we show the hyperradial functions for the three most important terms of this basis expansion. We focus in particular on the sensitivities to variations in the model space (panel a) and HO frequency (panel b). The interior part of the overlap is very well converged. However, we can observe that the expected exponential tail [23] is not reproduced. Increasing $N_{\max}$ we find that the tail builds up slowly. A similar behavior is found when varying the HO frequency, as can be seen from the hatched bands in Fig. 4(b). Small frequencies correspond to large oscillator lengths and therefore reproduce longer tails. However, a proper treatment of the continuum and long-range asymptotics is needed to describe this region more accurately. Such work is ongoing in the framework of the NCSM/Resonating Group Method (RGM) [34]. Note that the

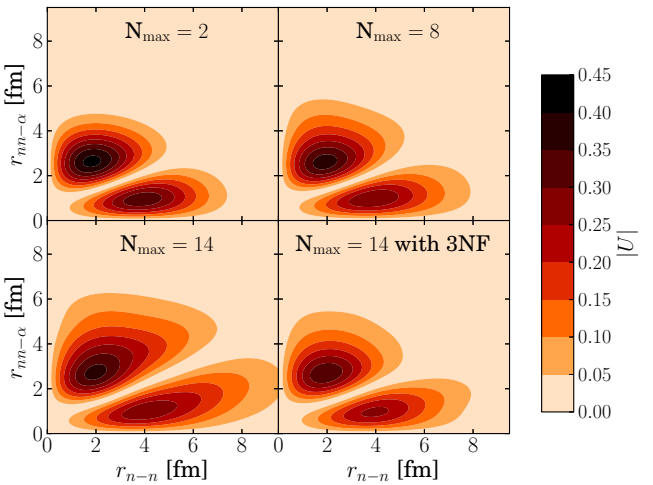

FIG. 3. (Color online) Model-space dependence of the three-body channel form factor $\langle {}^6\mathrm{He}(0^+)|{}^4\mathrm{He}(0^+)+n+n\rangle$. The main $L=S=0$ channel is shown for a sequence of calculations with increasing $N_{\max}$ performed with $\Lambda_{\mathrm{SRG}}=2.0$ fm^{-1} and $\hbar\Omega=16$ MeV. The lower right panel shows the same contour plot using an SRG-evolved chiral $NN+3N$F interaction [43].

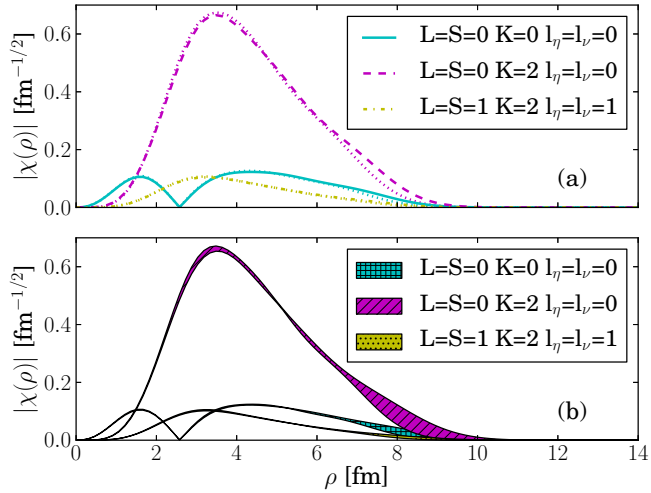

FIG. 4. (Color online) Hyperradial functions obtained from NCSM three-body channel form factors calculated with an SRG-evolved chiral two-body interaction ($\Lambda_{\mathrm{SRG}}=2.0$ fm^{-1}). (a) $N_{\max}$ dependence for a fixed frequency, $\hbar\Omega=20$ MeV. Thick lines correspond to $N_{\max}=14$ results, while dotted ones are $N_{\max}=12$. (b) A fixed model space ($N_{\max}=14$, shaded bands) and a range of HO frequencies, $\hbar\Omega=[16,22]$.

total norms of the hyperradial functions are determined mainly by the amplitude in the internal region, where the dependence on $N_{\max}$ and $\hbar\Omega$ is small. The relative weights of the five main components, as well as the total sum (i.e., the spectroscopic factor), are presented in Table II. The calculations are performed in the $N_{\max}=14$ model space for various SRG parameters and HO frequencies. We find that the sensitivity to variations in HO frequency and $N_{\max}$ is $\lesssim 1\%$. We note that we have very small variations around a total spectroscopic factor of ~ 1.3. The wave function obtained using a chiral $NN+3N$F Hamiltonian [43] displays an HH expansion that is qualitatively very similar. We have also computed the overlap with an excited core, $\langle {}^6\mathrm{He}(0^+)|{}^4\mathrm{He}(2^+)+n+n\rangle$. This channel corresponds to the first excited 2^+ state in the NCSM, situated just below the $2n+2p$ threshold but with slow energy convergence. Using $\Lambda_{\mathrm{SRG}}=2.0$ [fm]$^{-1}$, we find the total spectroscopic factor 0.30(4).

Conclusion and discussion. In this Rapid Communication we have derived expressions for translationally invariant core $+N+N$ overlap integrals starting from microscopic wave functions. We have used these overlap integrals to perform a microscopic investigation of the clustering of ^{6}He into $^4\mathrm{He}+n+n$. Large-scale *ab initio* NCSM calculations were performed with realistic nuclear interactions obtained from chiral perturbation theory. In addition, we used an SRG evolution to lower the resolution scale of the many-body Hamiltonian. We generated a series of such interactions, labeled by the SRG flow parameter, connected to each other by (approximately) unitary transformations. All of them reproduce the same two-nucleon, low-energy observables, but they have different high-momentum properties. This implies a resolution-scale dependence in the short-ranged part of the wave function. Therefore, we stress that the overlap integrals (and their norms, the spectroscopic factors) are not physical

TABLE II. Relative weights (in percent) of the HH expansion terms for the three-body channel form factor $\langle {}^6\mathrm{He}(0^+)|{}^4\mathrm{He}(0^+)+n+n\rangle$ calculated from NCSM wave functions. The last row shows the total spectroscopic factor.

Three-body channel			This work [Λ_{SRG} (fm^{-1}), $\hbar\Omega$ (MeV)]					With 3NF	Ref. [23]	Ref. [22]
K	$l_\eta = l_\nu$	$L = S$	(1.8,20)	(2.0,16)	(2.0,20)	(2.0,22)	(2.2,20)	(2.0,16)	(cluster)	(microscopic)
0	0	0	4.2	4.4	4.3	4.2	4.3	4.1	4.2	4.0
2	0	0	92.0	91.7	91.9	92.1	92.0	91.3	82.1	79.9
2	1	1	2.1	2.1	2.2	2.2	2.2	3.0	11.2	13.3
6	2	0	1.1	1.2	1.1	1.0	1.0	1.0	1.7	1.9
6	3	1	0.1	0.1	0.1	0.1	0.1	0.1	0.8	0.8
Spectroscopic factor:			1.3441	1.3263	1.3340	1.3391	1.3278	1.3284	0.9851	1.3957

observables [45,46]. In this work we have computed spectroscopic factors, as well as ground-state observables, using our series of Hamiltonians connected by SRG transformations.

In particular, we have studied the ground-state energy, two-neutron separation energy, and point-proton radius of ^{6}He. We employed published extrapolation schemes [39,40] to correct for the finite HO model space that were used in the computations, and we found a very consistent set of results for the energy while the extrapolation behavior of the radius calls for further studies.

Concerning the cluster structure of the ^{6}He ground state we have found that the total spectroscopic factor for $\langle {}^6\mathrm{He}(0^+)|{}^4\mathrm{He}(0^+)+n+n\rangle$ is significantly larger than one. In contrast, in phenomenological cluster models one assumes that this quantity is normalized to unity (see, e.g., the results of Ref. [23] in Table II). Our result is consistent with the translation-invariant shell-model upper limit of $25/16 \approx 1.56$ by Timofeyuk [21]. Furthermore, we have studied the $N_{\max}$ dependence of the overlap and could conclude that the clusterization is clearly driven by the Pauli principle. By performing an HH expansion of our three-body channel form factor, we found a strong dominance of the $K = 2$, $L = S = 0$ channel, which drives a two-peak structure in the T system of Jacobi coordinates. Furthermore, we can note that phenomenological approaches predict a significantly enhanced $L = S = 1$ channel as compared to our NCSM results with realistic, chiral interactions. We also find a non-negligible overlap with an excited core ^{4}He(2^+).

This work clears the path for further investigations of three-body clustering in light nuclei. Through the microscopically extracted overlap integrals we have a natural interface with reaction calculations that build on cluster degrees of freedom. In addition, we can combine this work with the ongoing development of the NCSM with continuum (NCSMC) [34]. The latter aims to couple NCSM A-body eigenstates with *ab initio* cluster wave functions. The formalism presented here will allow a detailed investigation of the resulting cluster structures.

Acknowledgments. The research leading to these results has received funding from the European Research Council under the European Community's Seventh Framework Programme (FP7/2007-2013)/ERC Grant Agreement No. 240603. This work was also supported by the Swedish Research Council (No. 2007-4078). This research used computational resources at Chalmers Centre for Computational Science and Engineering (C3SE) provided by the Swedish National Infrastructure for Computing (SNIC). We are much indebted to R. Roth for providing wave functions from the IT-NCSM and to Petr Navrátil, R. Wiringa, and N. Timofeyuk for insights and stimulating discussions on clustering in light nuclei.

[1] N. Austern, *Direct Nuclear Reaction Theories* (Wiley-Interscience, New York, 1970).
[2] K. Ikeda, N. Takigawa, and H. Horiuchi, Prog. Theor. Phys. Suppl. **E68**, 464 (1968).
[3] K. Wildermuth and Y. T'ang, *A Unified Theory of the Nucleus* (Vieweg, Braunschweig, 1977).
[4] J. Okołowicz, M. Płoszajczak, and W. Nazarewicz, Prog. Theor. Phys. Suppl. **196**, 230 (2012).
[5] B. R. Barrett, P. Navrátil, and J. P. Vary, Prog. Part. Nucl. Phys. **69**, 131 (2013).
[6] S. C. Pieper and R. B. Wiringa, Annu. Rev. Nucl. Part. Sci. **51**, 53 (2001).
[7] G. Hagen, T. Papenbrock, D. J. Dean, and M. Hjorth-Jensen, Phys. Rev. C **82**, 034330 (2010).
[8] W. Leidemann and G. Orlandini, Prog. Part. Nucl. Phys. **68**, 158 (2013).
[9] C. Ordóñez, L. Ray, and U. van Kolck, Phys. Rev. C **53**, 2086 (1996).
[10] P. F. Bedaque and U. van Kolck, Annu. Rev. Nucl. Part. Sci. **52**, 339 (2002).
[11] R. Machleidt and D. R. Entem, Phys. Rep. **503**, 1 (2011).
[12] E. Epelbaum, H.-W. Hammer, and U.-G. Meißner, Rev. Mod. Phys. **81**, 1773 (2009).
[13] S. K. Bogner, R. J. Furnstahl, and A. Schwenk, Prog. Part. Nucl. Phys. **65**, 94 (2010).
[14] K. M. Nollett, S. C. Pieper, R. B. Wiringa, J. Carlson, and G. M. Hale, Phys. Rev. Lett. **99**, 022502 (2007).
[15] S. Quaglioni and P. Navrátil, Phys. Rev. Lett. **101**, 092501 (2008).
[16] O. Jensen, G. Hagen, T. Papenbrock, D. J. Dean, and J. S. Vaagen, Phys. Rev. C **82**, 014310 (2010).
[17] C. Forssén, G. Hagen, M. Hjorth-Jensen, W. Nazarewicz, and J. Rotureau, Phys. Scr. T **152**, 014022 (2013).
[18] P. G. Hansen and J. A. Tostevin, Annu. Rev. Nucl. Part. S. **53**, 219 (2003).
[19] M. Macfarlane and J. French, Rev. Mod. Phys. **32**, 567 (1960).

[20] J. M. Bang, F. G. Gareev, W. T. Pinkston, and J. S. Vaagen, Phys. Rep. **125**, 253 (1985).
[21] N. K. Timofeyuk, Phys. Rev. C **63**, 054609 (2001).
[22] I. Brida and F. M. Nunes, Nucl. Phys. A **847**, 1 (2010).
[23] M. V. Zhukov, B. V. Danilin, D. V. Fedorov, J. M. Bang, I. J. Thompson, and J. S. Vaagen, Phys. Rep. **231**, 151 (1993).
[24] M. Brodeur *et al.*, Phys. Rev. Lett. **108**, 052504 (2012).
[25] L. B. Wang *et al.*, Phys. Rev. Lett. **93**, 142501 (2004).
[26] P. Mueller *et al.*, Phys. Rev. Lett. **99**, 252501 (2007).
[27] G. Papadimitriou, A. T. Kruppa, N. Michel, W. Nazarewicz, M. Ploszajczak, and J. Rotureau, Phys. Rev. C **84**, 051304 (2011).
[28] T. Neff and H. Feldmeier, Nucl. Phys. A **738**, 357 (2004).
[29] D. Baye, Y. Suzuki, and P. Descouvemont, Prog. Theor. Phys. **91**, 271 (1994).
[30] S. Korennov and P. Descouvemont, Nucl. Phys. A **740**, 249 (2004).
[31] E. Caurier and P. Navrátil, Phys. Rev. C **73**, 021302 (2006).
[32] S. Bacca, N. Barnea, and A. Schwenk, Phys. Rev. C **86**, 034321 (2012).
[33] S. C. Pieper, Riv. Nuovo Cimento **31**, 709 (2008).
[34] S. Quaglioni, C. Romero-Redondo, and P. Navrátil, Phys. Rev. C **88**, 034320 (2013).
[35] D. H. Gloeckner and R. D. Lawson, Phys. Lett. B **53**, 313 (1974).
[36] P. Navrátil, Phys. Rev. C **70**, 054324 (2004).
[37] L. Trlifaj, Phys. Rev. C **5**, 1534 (1972).
[38] S. A. Coon, M. I. Avetian, M. K. G. Kruse, U. van Kolck, P. Maris, and J. P. Vary, Phys. Rev. C **86**, 054002 (2012).
[39] R. J. Furnstahl, G. Hagen, and T. Papenbrock, Phys. Rev. C **86**, 031301 (2012).
[40] S. N. More, A. Ekström, R. J. Furnstahl, G. Hagen, and T. Papenbrock, Phys. Rev. C **87**, 044326 (2013).
[41] S. Bacca, A. Schwenk, G. Hagen, and T. Papenbrock, Eur. Phys. J. A **42**, 553 (2009).
[42] V. I. Kukulin, V. M. Krasnopol'Sky, V. T. Voronchev, and P. B. Sazonov, Nucl. Phys. A **453**, 365 (1986).
[43] R. Roth (private communication).
[44] M. Fabre de la Ripelle, Ann. Phys. (NY) **147**, 281 (1983).
[45] R. J. Furnstahl and H.-W. Hammer, Phys. Lett. B **531**, 203 (2002).
[46] R. J. Furnstahl and A. Schwenk, J. Phys. G: Nucl. Part. Phys. **37**, 064005 (2010).